Dynamic Behavior of Gentle Silty Slopes Based on Undrained Cyclic Shear Test

Jozef Jurko,[1)] Kyoji Sassa[2)] and Hiroshi Fukuoka[3)]
1) Research Centre on Landslides, Kyoto University, Gokasho, Uji, Kyoto 611-0011, Japan (jurko@landslide.dpri.kyoto-u.ac.jp)
2) Research Centre on Landslides, Kyoto University, Gokasho, Uji, Kyoto 611-0011, Japan (sassa@scl.kyoto-u.ac.jp)
3) Research Centre on Landslides, Kyoto University, Gokasho, Uji, Kyoto 611-0011, Japan (fukuoka@landslide.dpri.kyoto-u.ac.jp)

Abstract

Laboratory undrained cyclic shear behavior of silts has been studied by means of undrained cyclic stress - controlled ring shear tests. The dynamic behavior of silty soils on predetermined sliding surfaces in slopes with different gradients and various stress conditions were investigated. Four different initial stresses corresponding to slope angles (θ) of 0°, 10°, 15°, 20° were examined. As for seismic force that drives the slope downward a the driving cyclic shear stress with the constant amplitude according to simulated static conditions of a sliding surface was considered. Liquefaction potential of non-plastic silt and non-plastic silt — kaolinite mixtures along with potential of either limited or catastrophic deformations were evaluated. Furthermore, the loss of shear resistance and pore water build up in relation to a number of cycles was observed. For both non-plastic silt and silt of 5% clay content, there is the significant effect of the initial static driving shear stress on their dynamic behavior. An increase in an initial slope gradient is associated with an increase of the shear resistance similar to behavior of sands. Excess pore water pressure generated similarly for both non-plastic silt and silt of 5% clay content.

Keywords: landslides, silt, pore water pressure, liquefaction, undrained cyclic shear test

Introduction

Earthquake induced failures of slopes on shear surfaces consisting of saturated soils may result in high mobility landslides or flow type failures on the order of tens of meters. Associated with seismic risk evaluation there are many cases where limited deformations are tolerated, but the flow type of failures with long travel distances representing high mobility threat with catastrophic consequences in terms of damage and casualties are never permissible. Another type of phenomenon occurring during earthquakes known as soil liquefaction is very often directly connected with landslide processes, especially landslide mobility, resulting in large deformations. Many earthquake-induced landslides result from liquefaction phenomena, but many others simply represent the failures of slopes that were marginally stable under static conditions (Kramer, 1996). It should be noted that liquefaction phenomenon can be divided into two main groups: flow liquefaction and cyclic mobility. Both are very important and any evaluation of ground behavior during earthquakes should be considered carefully in both cases. Flow liquefaction can occur when shear stress required for static equilibrium of a soil mass is greater than shear strength of a soil in its liquefied state. Unlike flow liquefaction, cyclic mobility occurs when the static shear stress is less than the shear strength of the liquefied soil. In contrast to flow liquefaction, deformations produced by cyclic mobility are driven by both cyclic and static shear stresses. All of these deformations can occur on even very gentle slopes or on virtually flat grounds.

In particular, the loss of shear strength that may lead to large deformations and failures or even flow failures under moderate to high shear stresses of both flat and sloping grounds is the most important factor to understand the mechanism of catastrophic landslides.

Sassa (1996) conducted undrained cyclic loading ring shear tests to explain mechanism of Nikawa landslide. The Nikawa landslide in Hyogo prefecture, Japan, which was triggered by the January 1995 Hyogoken — Nambu earthquake showed a high mobility and killed 34 people in densely populated urban area. As Sassa (1996) reported, the sliding mass with a volume of 110 000–120 000 m^3 traveled over a distance 175 m. According to the field investigation, the landslide occurred on a gentle slope of about 20°. Based on experimental results the concept of sliding surface liquefaction was proposed to explain the gradual loss of shear resistance after failure due to the excess pore water pressure generation as a result of grain crushing with progress of shear displacement. It was found that sliding surface liquefaction took place along the sliding surface and was

pp. 411–420

responsible for low apparent friction angle of rapid and long traveling landslides.

Several other landslides triggered on gentle slopes were reported from the last earthquakes in Japan. During the 2004 Mid-Niigata Prefecture earthquake, thousands of landslides were triggered, among them two large-scale rapid landslides (Higashi Takezawa and Terano landslides) occurred within the area of past landslide masses and dammed the river at the toe of the landslides, posing great risks for the society (Sassa et al., 2005). Based on detailed field investigation it was found that both large-scale rapid landslides Higashi Takezawa and Terano landslides fall within the category of gentle slopes (i.e. $\leq 20°$). These landslides represent an evidence of large deformations and failures in silty — sandy materials.

For many years, liquefaction related processes and failures were thought to be limited to sands. A comprehensive amount of studies have been made for developing the methodology to assess liquefaction potential of sands. Recently, the influence of fines on dynamic behavior of sands has attracted attention of researchers and a number of studies can be found. As stated by Bolulanger and Idriss (2004) the situation is, however, more complicated for low-plasticity silts and clays that are near the transition between sand-like and clay-like behavior. Fine grained soils were considered unable of pore water generation, which is directly responsible and associated with soil liquefaction. Nevertheless, many natural soils contain a certain amount of fines (particle size less than 0.074 mm) or are formed of fine grained soils. Kishida (1969) reported liquefaction of soils with up to 70% fines and clay fraction of 10% during Mino-Owar, Tohankai and Fukui earthquakes. Yilmaz et al. (2004) reported a significant deformations of the city Adapazari — Turkey after 1999 Kocaeli earthquake, where study sites predominately consisted of fine grained surface soils of low plastic silt — clay mixtures. Wang and Sassa (2002) concluded that not only sandy, but also silty materials exhibit liquefaction behaviour in fully saturated undrained conditions under monotonic loading. Youd et al. (1985) reported liquefaction of silt - clay materials at the Whiskey Spring during Idaho earthquake of 1983.

Approach

To evaluate and mitigate hazards associated with seismically induced liquefaction and consequent deformations in silty soils, better knowledge of their seismic behavior is needed. In this study, the undrained cyclic shear behavior of silt has been studied by means of undrained cyclic stress — controlled ring shear tests. To investigate cyclic behavior of silty slopes within a range of 0 to 20 degrees, undrained cyclic shear tests were conducting on a predetermined sliding surface. In particular effects of initial stresses corresponding to simulated static conditions of a sliding surface on excess pore water pressure generation and shear resistance reduction known as either liquefaction or cyclic mobility were thoroughly investigated. Furthermore, the loss of shear resistance and pore water build up in relation to number of cycles was observed. The last, but not the least the effect of clay particles on cyclic shear behavior of silt was examined. Accurate investigation of the undrained cyclic behavior of silts and clays with varying levels of plasticity has been the subject of the present research. This study covers only beginning of the widely defined problem related to dynamic behavior of non-plastic silt and its variations to plastic clay. To better understand undrained cyclic behavior of silt governed by a little change of clay content, two different blended silt mixtures were achieved by mixing of non-plastic silt with 0 and 5% of kaolinite clay respectively. Prakash and Puri (2003) stated if small portion of clay is added into a sample of non-plastic silt two cases of behavior in terms of excess pore water pressure origin are expected to happen. Firstly, excess pore water pressure may increase as a consequence of reduced hydraulic conductivity caused by adding a portion of clay. Secondly, clay particles may impart some plasticity to the soil which may increase resistance to liquefaction. In addition, potential of catastrophic landslides associated with liquefaction phenomenon was analyzed.

When assessing liquefaction potential and related cyclic failures in sloping grounds the soil element is subjected to the static shear stress maintained all the time, before during and after an earthquake shaking. Then, in the analysis measured shear resistance under a certain given number of cycles is compared against the seismically induced driving shear stress. Comparison of these two variables determines prerequisite for whether or not liquefaction is triggered or either large deformation or limited deformation takes place. Evaluating post-failure behavior, it is worth comparing the initial sustained static shear stress against shear strength of the soil which was mobilized after enough large deformation with no further significant changes. This strength stands for residual strength of a soil. Relationship in between the initial driving static shear stress and undrained resistance of the soil on a sliding surface defines whether a catastrophic landslide occurs or not. The catastrophic large displacement is observed when the static driving shear stress exceeds shear strength at a residual state.

Based on mentioned above, dynamic behavior of silty soils on predetermined sliding surfaces in slopes with different gradients and various stress conditions were investigated. Four different initial stresses corresponding to slope angles (θ) of 0°, 10°, 15°, 20° were examined. As for seismic force that drives the slope downward a driving cyclic shear stress with constant amplitude according to simulated static conditions of a

sliding surface was considered. Liquefaction potential of non-plastic silt and non-plastic silt — kaolinite mixtures along with potential of either limited or catastrophic deformations were evaluated. The term catastrophic deformation is assumed to occur when residual shear strength is smaller as compared to the static driving shear stress accompanied by an unlimitedly large displacement.

Initial conditions

Similar to the study by Trandafir and Sassa (2005) both the initial total normal stress σ_0 and the initial driving shear stress τ_0 acting on a sliding surface, corresponding to simulated conditions prior to the earthquake can be derived from infinite slope using normal and tangential components of W, of a soil column of width b, involving desired inclination (Fig. 1). Equations can be written as follows:

$$\sigma_0 = \gamma H \cos^2 \theta \quad (1)$$

$$\tau_0 = \gamma H \sin\theta \cos\theta \quad (2)$$

Where H is the height of the soil mass above the sliding surface and γ is the average unit weight of the soil within the sliding mass.

Similarly, the seismic components of total normal stress, $\Delta\sigma$, and driving shear stress, $\Delta\tau_d$, on the sliding surface due to horizontal seismic force provided by cyclic loading can be expressed as follows:

$$\Delta\sigma = k\tau_0 \quad (3)$$

$$\Delta\tau_d = k\gamma H \cos^2 \theta \quad (4)$$

Where k is the horizontal coefficient of earthquake acceleration. Then, the dynamic total normal stress, σ, and the driving shear stress, τ_d, on the sliding surface at a certain point during an earthquake will be given by the following equations:

$$\sigma = \sigma_0 - \Delta\sigma \quad (5)$$

$$\tau_d = \tau_0 + \Delta\tau_d \quad (6)$$

Four different initial stresses corresponding to slope angles (θ) of 0°, 10°, 15° , 20° were examined under the initial effective normal stress of 200 kPa for samples with 0% of kaolinit and 150 kPa for mixtures with 5% of clay. The driving cyclic shear stress with constant amplitude according to simulated static conditions of the sliding surface was applied.

Samples were prepared from two soils Silica sand No. 8 (S8) and kaolinite. Clean S8 and its mixtures with 5% of kaolinite by weight were considered on the predetermined sliding surface. As for mineral composition, Silica sand no. 8 is mainly formed of sub angular and angular quartz and is commercially available for construction purposes. The grain size distribution of S8, illustrated in Fig. 2 shows that the sand is uniform with the grain size ranging from 0.001 to 0.4 mm with more than 70% by dry weight of fine grains. The mean diameter is 0.05 mm and the maximum and minimum dry densities are 1.44 and 0.99 g/cm^3, respectively. Kaolinite is by far the most common and most clay deposits contain at least some kaolinite. Along with other clay minerals of kaolinite group, forms from the alteration (mostly weathering) of aluminium rich silicate minerals such as feldspars.

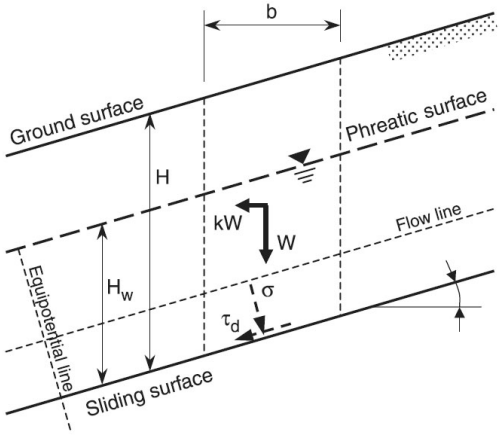

Fig. 1. Infinite slope conditions

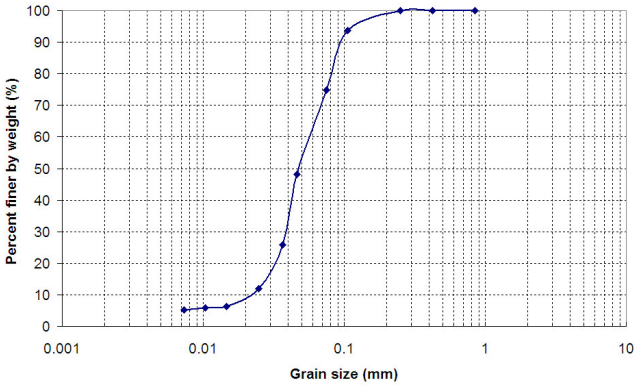

Fig. 2. Grain size distribution of S8

Experimental procedure

Ring shear apparatus

Ring shear apparatus was initially developed to investigate residual shear resistance mobilized along the sliding surface following large shear displacements in landslides of high mobility. The test configuration for the ring shear device was introduced by Hvorslev (1939) in. This principle was adopted and improved by Bishop et al. (1971), Bromhead (1979), Savage and Sayed (1984), Hungr and Morgenstern (1984), Tika (1989) and Garga and Sendano (2002) as stated in Sassa (2004).

A series of ring shear apparatus has been developed and improved (Sassa, 1997; 2000); the version DPRI Ver.5 — intelligent, undrained, torque-controlled ring shear apparatus (Sassa et al., 2003) was used in this study. The general purpose of the DPRI ring-shear testing program is to use apparatus that can quantitatively simulate the entire process of failure of a soil sample, from initial static or dynamic loading, through shear failure, pore-pressure changes and possible liquefaction, to large-displacement, steady-state shear movement. Schematic diagram of the concept of using ring shear apparatus is shown in Fig. 3. Current undrained ring-shear apparatus geotechnically simulates the formation of the shear zone and the post-failure mobility of high-speed landslides and observes the consequence of mobilized shear resistance, as well as the post-failure shear displacement and generated pore-water pressure. It is proved that undrained torque-controlled ring shear apparatus is capable to simulate and observe all the parameters in terms of stated goals of this investigation.

A scheme of the DPRI-Ver.5 ring shear as described in Agung et. al., (2004) is shown in Fig. 4. The specimen is placed in the donut-like (circular) form between the inner and the outer stainless steel shear boxes. The outer diameter of the shear box is 18.0 cm and the inner diameter is 12.0 cm, therefore the area of shear surface is approximately 141.4 cm^2. The specimen is sheared by rotating the lower half of the shear box (rotatable part in Fig. 4a), while two resistance transducers restrain the upper half of the shear box (in the left and right arms of the ring shear box in Fig. 4b) with which shear resistance is measured. Both of speed-controlled and torque-controlled tests are possible with this apparatus. A rubber edge is bonded to the upper surface of the lower half of the shear box in order to prevent leakage of water and specimen during consolidation and undrained shearing. Detail information about the structure of this apparatus and its operation principles can be found elsewhere (Sassa, 2004).

Sample preparation and test procedure

The dry deposition method was used in this study to place the sample into the shear box. Test procedure of test preparation for ring shear apparatus is similar as described in Sassa et al. (2003). After oven dried sample was placed into the shear box, CO_2 was supplied to remove remaining air. Afterwards, de-aired water was allowed to percolate slowly throughout the specimen to complete saturation. The degree of saturation was checked by measuring B_D value (Sassa, 1985).

$$B_D = \Delta u / \Delta \sigma \tag{7}$$

Where Δu is the increment of pore water pressure increase due to a change in total normal stress in undrained conditions. For each test B_D value *geq* 0.95 was measured what implies fully saturated specimen. All samples were normally consolidated under the effective normal stress of 200 kPa for non-plastic silt and 150 kPa for silt-clay mixtures respectively. After consolidation at the initial effective normal stress, the initial driving shear

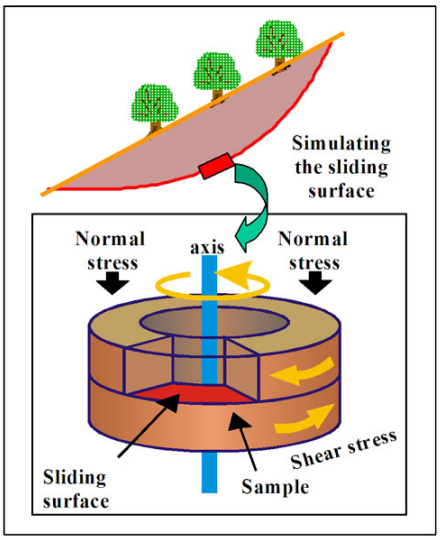

Fig. 3. Concept of using ring shear apparatus

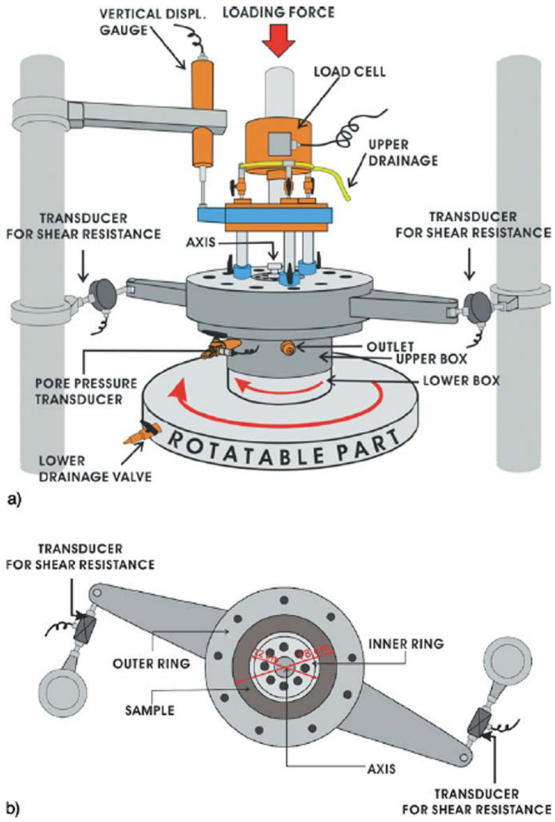

Fig. 4. A scheme of DPRI-Ver.5 ring shear

stress was increased reaching value in accordance with calculated and simulated static conditions on the sliding surface. Afterwards, the shear box was switched to undrained conditions, the driving cyclic shear stress with constant amplitude was applied corresponding to CSR = 0.5. (CSR= $\Delta\tau_d/\sigma'_0$) with a loading frequency of 0.5 Hz.

Test results and discussion

Undrained cyclic behavior of non-plastic silt

Based on stated goals of this study, a series of undrained cyclic shear test was conducted on the predetermined sliding surface formed of non-plastic silt (S8) and its mixture with 5% of kaolinite by weight. In particular, effects of initial stresses corresponding to simulated static conditions of the sliding surface on excess pore water pressure generation and shear resistance reduction in four different slope gradients were examined. Table 1 summarizes characteristics of simulated slopes where the sliding surface is formed of non-plastic silt. Specimens containing 5% of kaolinite (designation A5-D5) and related test conditions are presented in Table 2. It should be noted e_0 stands for void ratio after consolidation right before an experiment began. H (m) represents the height of the soil mass above the sliding surface.

In the diagram of Fig. 5 typical results are presented depicting time series data of normal stress, shear stress and pore water pressure of slope D. As can be seen cyclic loading generated excess pore water pressure very quickly to a value of about 65% of total normal stress in its 4^{th} cycle. As soon as the experiment began the sample failed and shear resistance decreased gradually with an increase a number of cycles. Since the cyclic driving shear stress was greater than mobilized shear resistance a large deformation of the slope was observed with liquefaction potential to occur, however pore water pressure did not rise up more so that no liquefaction was reproduced. Although pore water pressure increased slowly after it reached its maximum in 4th cycle, shear resistance decreased gradually with a progress of shear displacement and culminated in steady state strength smaller than the initial driving shear stress. As soon as post-failure strength gained a value of the initial static driving shear stress, shear displacement accelerated rapidly, pore water pressure increased slowly and sample failed by mode of a flow slide. Similar cyclic response with progress of shear displacement in mode of a catastrophic slide was produced in tests designated as D5 and marginally C5. Inspection of C5 test results revealed that shear resistance gradually reduced very close to a value of the initial sustained shear stress and further degradation was not observed, even though pore water pressure slowly accumulated. Specimens

Table 1. Characteristics of simulated slopes (non-plastic silt)

Slope	θ (°)	H (m)	σ'_0	tan θ	e_0
A	0	10.0	200	0.00	1.16
B	10	10.4	200	0.18	1.14
C	15	10.6	200	0.26	1.18
D	20	11.4	200	0.36	1.16

Table 2. Characteristics of simulated slopes (5% kaolinit content)

Slope	θ (°)	H (m)	σ'_0	tan θ	e_0
A5	0	8.8	150	0.00	1.10
B5	10	9.1	150	0.17	1.22
C5	15	9.5	150	0.27	1.11
D5	20	10.0	150	0.36	1.09

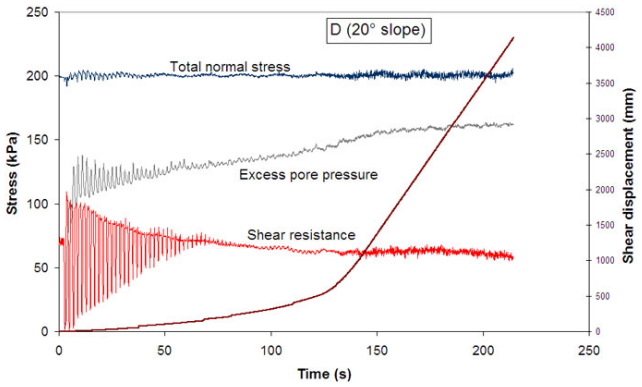

Fig. 5. Typical test results from undrained cyclic stress — controlled ring shear tests

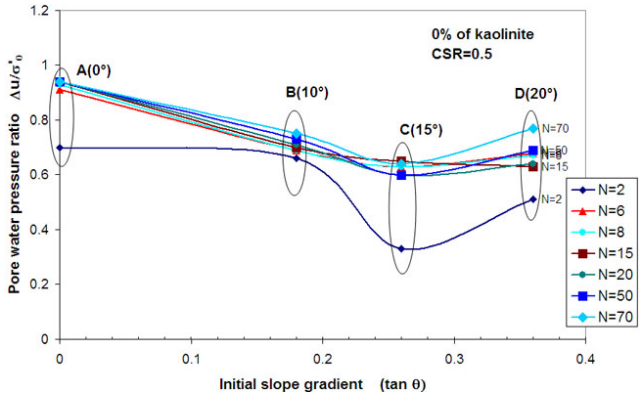

Fig. 6. Initial slope gradient — excess pore water pressure ratio relationship in terms of cycle numbers for non-plastic silt

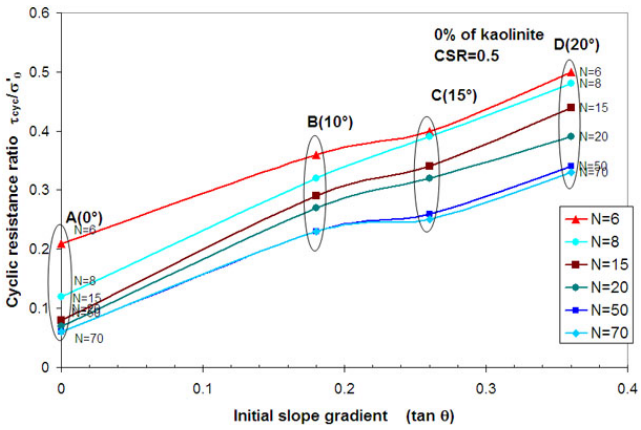

Fig. 7. Initial slope gradient — cyclic resistance ratio relationship with respect to a number of cycles for non-plastic silt

presented on sliding surfaces of other simulated tests exhibited deformations and limited shear displacements governed by the applied driving shear stress.

An important issue of the concern in this study was to investigate the effect of initial shear stresses corresponding to gentle slopes (0–20°) on dynamic behavior of silt assuming on the potential sliding surface. An attempt was to examine several different initial shear stresses of silty soils presented on the sliding surface subjected to cyclic loading. The effect of the initial shear stress is clearly seen in Fig. 6 where the test results are presented in terms of the initial slope gradient against pore water pressure ratio defined as the ratio of maximum pore water pressure in particular cycle to the initial effective normal stress with respect to a number of cycles. The presented test [JJ1]results show, that excess pore water pressure generated relatively quickly. After 15 cycles of loading about 65% of the normal stress was exceeded in all the cases, yet only in case of flat ground excess pore water pressure reached a value of 90–95% of the normal stress. The increase in pore water pressure generation is more rapid at lower cycle number. This is similar to the behavior of sand subjected to cyclic loading. The obvious trend is seen; the higher initial slope gradient the smaller amount of excess pore water pressure generated. In addition, the loss of shear resistance represented by cyclic resistance ratio (CRR) with respect to the initial slope gradient encompassing a number of cycles was ascertained (Fig. 7). In this study, CRR is defined as the ratio of maximum shear resistance in 50^{th} cycle to the initial effective normal stress. As can be seen from the diagram, an increase in the initial slope gradient resulted in an increase of cyclic resistance ratio, similarly as it is believed for sands (Vaid and Chern, 1983[JJ2]). The reduction of cyclic shear resistance was small for liquefaction to occur except the case of flat ground. As for the shear strength reduction concerning a number of cycles it can be concluded that shear resistance decreased approximately evenly for each of our tests. The influence of 5% of kaolinit on dynamic behavior of the silty sliding surface was studied and results are summarized in Fig. 8 and Fig. 9.

Excess pore water pressure demonstrated similar progress as for pure silt, nevertheless its development

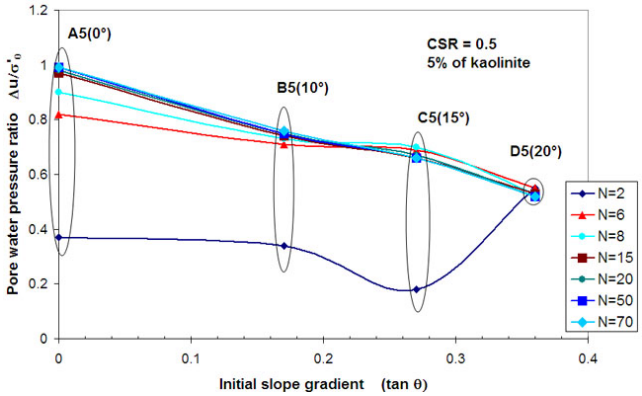

Fig. 8. Initial slope gradient — excess pore water pressure ratio relationship in terms of cycle numbers for a mixture with 5% of kaolinit content

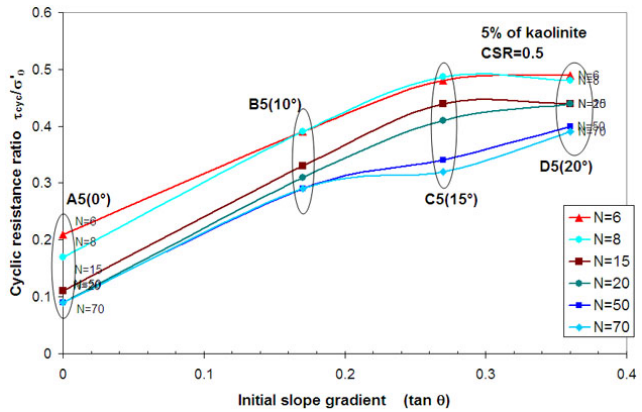

Fig. 9. Initial slope gradient — cyclic resistance ratio relationship with respect to a number of cycles for a mixture with 5% of kaolinit content

in terms of a number of cycles was slightly retarded, but the final state was about the same. A higher pore water pressures are achieved at lower cycle number. A noticeable difference was discovered comparing both experiments on 20° slope simulation (Fig. 8, 9). The sample with 5% of clay content experienced a little bit smaller pore water pressure generation than sample without clay mineral. Similarly to test D shear strength decreased gradually with progress of shear displacement in a mode of a catastrophic slide. Generally, for both non-plastic silt and silt of 5% clay content, there is the significant effect of the initial static driving shear stress. An increase in the initial slope gradient is associated with an increase of shear resistance.

Conclusions

The following conclusions can be drawn based on the experimental results: Dynamic behavior of silty soils on predetermined sliding surfaces in slopes with different gradients and various stress conditions were investigated by means of undrained cyclic stress — controlled ring shear tests. Four different initial stresses corresponding to slope angles (θ) of 0°, 10°, 15° and 20° were examined. Mainly the effect of initial stresses corresponding to simulated static conditions and clay content on excess pore water pressure generation and the shear resistance reduction leading to a catastrophic flow slides was evaluated. Fig. 10, 11 summarize the obtained results.

1. For both non-plastic silt and silt of 5% clay content, there is the significant effect of the initial static driving shear stress on their dynamic behavior. A clear trend is shown in Fig. 10, 11 for effects of initial slope gradient and clay mineral content (kaolinite) on the cyclic behavior of silty — clayey soils on the potential sliding surface. The increase in the initial slope gradient is associated with an increase of shear resistance similar to behavior of sands. The reduction of cyclic shear resistance in all of our tests was small for flow liquefaction to occur except the cases of flat ground, test A5 and A.

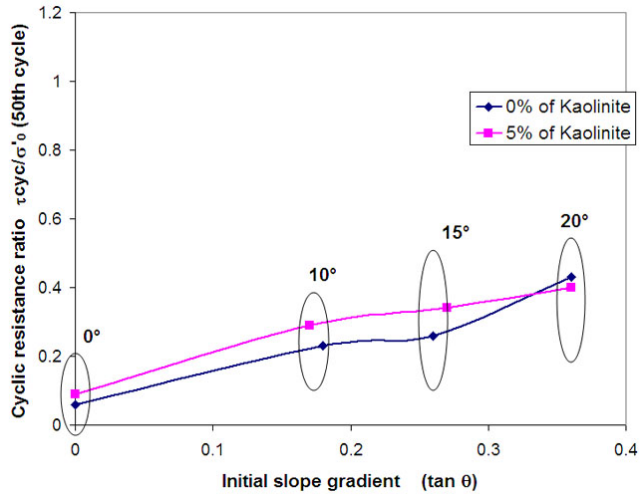

Fig. 10. Initial slope gradient — shear resistance ratio relationship

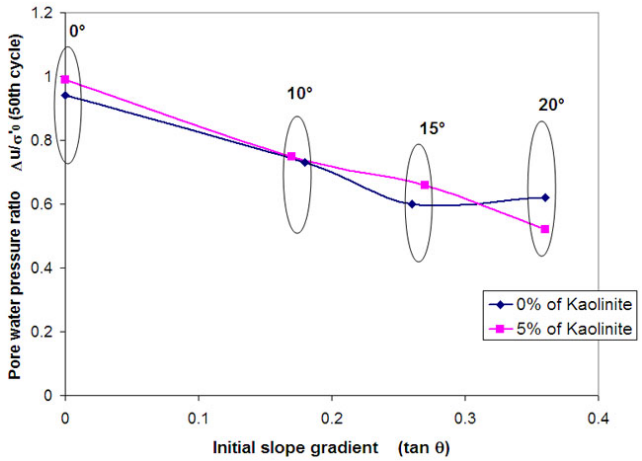

Fig. 11. Initial slope gradient - excess pore water pressure ratio relationship

2. The addition of 5% of kaolinite by weight resulted in the very slight increase of shear resistance for all the tests except of D5 and D, where an opposite effect was observed. In general, the difference was enough small and for approximate evaluation can be neglected.
3. Excess pore water pressure generated similarly for both non-plastic silt and silt of 5% clay content. It implies that addition of 5% of kaolinite had no significant effect on the generated pore pressures for all simulated initial slope gradients. Obviously, plasticity of non-plastic silt and its 5% clay mixture remained nearly constant. An obvious trend is seen; the higher initial slope gradient the smaller amount of excess pore water pressure generated.
4. The increment of pore water generation is distinct at lower cycle numbers. As for the shear strength reduction concerning to a number of cycles it can be concluded that shear resistance decreased approximately evenly with an increase of a cycle number for each of our tests.
5. Remembering principles already mentioned above, silty material on each of our simulated sliding surfaces underwent significant deformations resulting in likely damages. Two cases (0%, 5% of clay content) of experimental simulation related to the initial slope gradient of 20° and marginally 15° slope exhibited failure by mode of a catastrophic flow slide.
6. This study covers only beginning of the comprehensive research related to dynamic behavior of non-plastic silt and its variations up to plastic clay.
7. It can be concluded, that a further study on low-plasticity silts and clays near the transition between sand-like and clay-like behavior is needed.
8. Present outcomes along with results of future investigation can be used for both, engineering procedures evaluating the undrained seismic behavior of silty soils and numerical methods for computer simulations.

Acknowledgement

These tests were conducted at Research Centre on Landslides at Kyoto University. The support of the centre is gratefully acknowledged.

References

Agung, M.W., Sassa, K., Fukuoka, H. and Wang, G. (2004) Evolution of Shear-Zone Structure in Undrained Ring-Shear Tests. *Landslides*, **1**(1), 101–112

Boulanger, W.R. Idriss, I.M. (2004) Evaluating the potential for liquefaction or cyclic failure of silts and clays. Report No. UCD/CGM-04/01, Center for Geotechnical Modeling, University of California, Davis.

Kishida, H. (1969) Characteristics of Liquefied Sand during Mino-Owari, Tohnankai, and Fukui Earthquakes. *Soils and Foundations*, **3**(2)

Kramer, S.L. (1996) *Geotechnical earthquake engineering.* Prentice-Hall, Inc., Upper Saddle River, N.J., p. 653.

Prakash, S. and Puri, V.J. (2003) Liquefaction of silts and silt-clay mixtures. Internet

Sassa, K. (1985) The mechanism of debris flows. *In* Proceedings of the 11th International Conference on Soil

Mechanics and Foundation Engineering, San Francisco, Calif., 12–16 August 1985. A.A. Balkema, Rotterdam, The Netherlands. Vol. **3**, pp. 1173–1176

Sassa, K. (1996) Prediction of earthquake induced landslides. Special lecture of 7th International Symposium on Landslides, "*Landslides*", Rotterdam, Balkema, **1**, 115–132.

Sassa, K. (1997) A New intelligent type dynamic loading ring shear apparatus. Landslide News (Japanese Landslide Society), No. 10, p. 33

Sassa, K. (2000) Mechanism of flows in granular soils. *GeoEng 2000*, Vol. **1**: Invited Papers, 1671–1702

Sassa, K., Wang, G.H. and Fukuoka, H. (2003) Performing undrained shear test on saturated sands in a new intelligent ring shear apparatus. *ASTM Geotechnical Testing Journal*. Vol. **26**, No. 3, 257–265

Sassa, K., Fukuoka, H., Wang, G. and Ishikawa, N. (2004) Undrained dynamic-loading ring-shear apparatus and its application to landslide dynamics. *Landslides*, **1**(1), 7–19

Sassa, K. (2005) Dynamic properties of earthquake-induced large scale rapid landslides within past landslide masses. *Landslides*, **2**(2), 125–134.

Trandafir, A.C. and Sassa, K. (2005) Seismic triggering of catastrophic failures on shear surfaces in saturated cohesionless soils. *Canadian Geotechnical Journal*, **42**(1), 229–251

Vaid, Y.P. and Chern, J.C. (1983) Effect of static shear on liquefaction of sands, *Soil and Foundations*, **23**(1), 47–60

Wang, F.W., Sassa, K. and Fukuoka, H. (2000) Geotechnical simulation test for the Nikawa landslide induced by January 17, 1995 Hyogoken-Nambu earthquake. *Soils and Foundations*, **40**(1), 35–46.

Wang, G. and Sassa, K. (2002) Post-failure mobility of saturated sands in undrained load-controlled ring shear tests. *Canadian Geotechnical Journal*, **39**(4), 821–837.

Yilmaz, M.T., Pekcan, O. and Bakir, B.S. Undrained cyclic shear and deformation behavior of silt - clay mixtures of Adapazari, Turkey. *Soil Dynamics and Earthquake Engineering* **24**, 497–507

Youd, T.L., Harp, E.L., Keefer, D.K. and Wilson, R.C. (1985) The Borah Peak, Idaho Earthquake of October 28, 1983 — Liquefaction. *Earthquake Spectra, Earthquake Engg. Res. Inst.*, **2**(1), 71–89